

Transport Properties of Layered Cuprate Films and Superconducting Superlattices with Fluorite-Type Block Layers

Sumio Ikegawa, Yuichi Motoi, and Masao Arai*

Advanced Materials & Devices Lab., Corporate R & D Center, Toshiba Corp., Kawasaki 212-8582, Japan.
Fax: 81-44-520-1801, e-mail: sumio.ikegawa@toshiba.co.jp

*Advanced Materials Lab., National Institute of Materials Science, Tsukuba, Ibaraki 305-0044, Japan
Fax: 81-298-52-7449, e-mail: arai.masao@nims.go.jp

We tried to control an atomic layer structure and, consequently, the transport properties in layered cuprates. In $(\text{Pb}_2\text{Cu})\text{Sr}_2\text{Dy}_x\text{Ce}_{n-x}\text{Cu}_2\text{O}_{2n+6}$ (Pb-32 n 2 phase: $n=3-8$), the distance, d , between a pair of CuO_2 planes can be changed with a unit thickness of 0.28 nm by changing the number, n , of the atomic layer in the fluorite block layer. Thin films of this family were grown by atomic layer-by-layer molecular beam epitaxy. Transport properties of Pb-32 n 2 phases have been studied and discussed in comparison with the *ab initio* electronic structure calculations. Using this family, we have successfully grown $[(\text{Pb-32}n2)_1(\text{Pb-3212})_3]_9$ ($n=3, 4, 6$) superconducting superlattices in which the distances between the superconducting layers are controlled at the shortest intervals so far achieved. In these superlattices, as expected, the activation energy of flux motion decreases with increasing n .

Key words: superconductivity, layered cuprate, MBE, vortex dynamics

1. INTRODUCTION

The high- T_c superconductors can be regarded as stacks of intrinsic Josephson junctions, because of their layered crystal structure.¹ The intrinsic junctions offer high performance, such as high $I_c R_N$ product and SIS tunnel characteristics. However, the series array of the same junctions alone is of limited use for electronic applications: technologies for making thick superconducting electrodes beside the junctions or for making a single junction at any place are needed. Thus, the control of Josephson coupling in the arbitrary unit cell of layered cuprates is desirable in electronic applications. This should be accomplished by the artificial modification of an atomic layer stacking in the layered crystal structure.

In $(\text{Pb}_2\text{Cu})\text{Sr}_2(\text{Ln}, \text{Ce})_n\text{Cu}_2\text{O}_{6+2n-2}$ ($n>2$, Ln=rare earth element) (Pb-32 n 2 phase), the distance between a pair of CuO_2 planes across an insulating fluorite-type layer can be arbitrarily chosen. So, the Pb-32 n 2 family offers the potential to control electronic anisotropy or the strength of Josephson coupling along the c -axis.² We have successfully grown epitaxial films of Pb-32 n 2 with $n=3-8$ by the atomic layer-by-layer molecular beam epitaxy (MBE) technique.² The Pb-32 n 2 phases with $n>4$ are essentially impossible to obtain in pure phase form with other techniques, since all these phases are energetically very close.

In the first half of this paper, we report the in-plane transport properties of Pb-32 n 2 films with $n=3$ and 5. The objective of this study is to understand how the carriers are doped by cation substitution and to investigate how transport properties are affected by changing the distance, d , between a pair of CuO_2 planes.

The Pb-32 n 2 phases with $n>2$ have not exhibited superconductivity to date. Thus, we have made multilayers of the Pb-3212 superconductor and Pb-32 n 2

phase to investigate how the anisotropy of superconductivity is affected by changing the distance, d .

Taking advantage of the naturally layered structure, high- T_c multilayer structures have been extensively studied.³ They offer the possibility of modifying in a systematic way some specific properties of high- T_c superconductors, such as vortex dynamics. A variety of superlattices have been reported, such as $\text{YBa}_2\text{Cu}_3\text{O}_7/\text{PrBa}_2\text{Cu}_3\text{O}_7$ (YBCO/PBCO), $\text{Bi}_2\text{Sr}_2\text{CaCu}_2\text{O}_8/\text{Bi}_2\text{Sr}_2\text{Cu}_2\text{O}_6$, and $\text{YBa}_2\text{Cu}_3\text{O}_7/\text{SrRuO}_3$. In these superlattices, the thickness of the spacer material was restricted to an integral multiple of the c -axis length, for example, 1.2 nm for PBCO. The shortest unit length was a lattice parameter of a perovskite primitive cell (~ 0.39 nm).

In the latter part of this paper, we report on the superlattices in which the distances between the superconducting layers are controlled at the shortest intervals so far. This was achieved by using the Pb-32 n 2 family. We discuss how the interlayer coupling was changed depending on n .

2. EXPERIMENTS

The $(\text{Pb}_2\text{Cu})\text{Sr}_2\text{Dy}_x\text{Ce}_{n-x}\text{Cu}_2\text{O}_{2n+6-2z}$: $n=3$ and 5 thin films were grown by sequential deposition using the MBE apparatus. Pb, Sr, Dy, Ce, Ca, and Cu metals were evaporated from the effusion cells onto a $\text{SrTiO}_3(001)$ surface. During growth, pure ozone gas was supplied to the substrate and the substrate temperature was kept constant at 943 K to 973 K. We have also synthesized superlattices of alternating one-unit-cell-thick layers of Pb-32 n 2 ($n=3, 4, 6$) with three-unit-cell-thick layers of Pb-3212, which are expressed as $[(\text{Pb-32}n2)_1(\text{Pb-3212})_3]_9$. The crystal structure of one cycle is shown in Fig. 1.

After the film growth, the phases present and the lattice parameters were determined by x-ray diffraction

(XRD), using Cu- $K\alpha$ radiation. Resistivity measurements were carried out by a conventional dc four-probe method in the temperature ranged between 1.5 K and 300 K. Resistivity was also measured under an applied field using a 10-T superconducting solenoid. The sample temperature was measured by using a calibrated Cernox thermometer. The sample holder could be rotated relative to H with an accuracy better than 0.1° . Thermoelectric power was measured by a steady-state technique at temperatures between 40 K and 300 K. The hole density, p , per $[\text{CuO}]^{2p}$ was estimated from the room-temperature thermopower, S_{290} , using Tallon's universal relation⁴ between S_{290} and p .

3. RESULTS AND DISCUSSION

3.1 Pb-32n2 phase with $n=3, 5$

The XRD experiments confirm that the films have a single-phase Pb-32n2 structure with $n=3$ or 5, and the c -axis of the films was perpendicular to the substrate surface.

In-plane transport properties of the Pb-3252 phase films [nominal compositions: $(\text{Pb}_2\text{Cu})\text{Sr}_2\text{Ce}_{5-x}\text{Dy}_x\text{Cu}_2\text{O}_{16-z}$] are shown in Fig. 2. From the simple calculation of the valence assuming $z=0$ and $\delta=0$, p would increase with Dy concentration, x , following the relation $p=(x-1)/2$. The experimental results of thermopower in Fig. 2 (b) were used to estimate p . A slight increase in

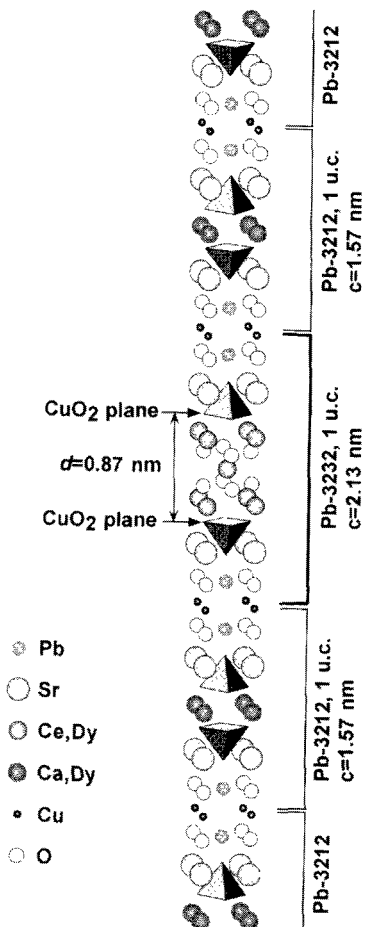


FIG. 1. Crystal structure of one cycle of $[(\text{Pb-3232})_1(\text{Pb-3212})_3]_9$ superlattices.

p with x was observed from $p=0.0831$ for $x=0.97$ to $p=0.0891$ for $x=1.86$. The substitution of Ce^{4+} by Dy^{3+} in the fluorite block increased the hole density, but the efficiency of hole doping was lower than the expectation from the simple calculation of the valence. This is common to the Pb-3232 and Pb-3252 phases.⁵

One of the reasons for the low efficiency may be that the substitution of Ce^{4+} by Dy^{3+} creates compensating oxygen vacancies. Recently, the electronic structures of the Pb-3222 and Pb-3232 phases were calculated within the local-density approximation for the first time and were compared with those for the Pb-3212 phase.⁶ Possible mechanisms for the low efficiency of hole doping were revealed by the calculations. The substitution of Ce^{4+} by Ln^{3+} lifts the energy level of the oxygen in the fluorite block. As a result, the oxygen atoms become unstable and the oxygen vacancies in the fluorite block may increase.⁶ If the creation of oxygen vacancies is prevented by, for example, high-pressure oxygen treatment, the substitution with $x>2$ brings about the contribution of the oxygen $2p$ orbital in the fluorite block to the density of states at Fermi energy. It means that a portion of doped holes are not released to the CuO_2 planes but are trapped in the fluorite blocks.⁶ These effects are likely to be crucial to superconductivity and transport properties in all the layered cuprates having a fluorite block, and further studies are required in order to clarify this point.

Resistivity measurements showed no evidence of superconductivity for the Pb-3232 and Pb-3252 phases. Instead, the weak localization behavior was observed, for example, in the case of the sample with $x=1.86$ at temperatures below 60 K in Fig. 2 (a). The sheet conductance per CuO_2 plane was estimated from the resistivity data and was similar for the Pb-3232 phase and Pb-3252 phase.⁵ This means that the strength of localization does not increase when the distance between a pair of CuO_2 planes, d , increases from 0.87 nm to 1.44

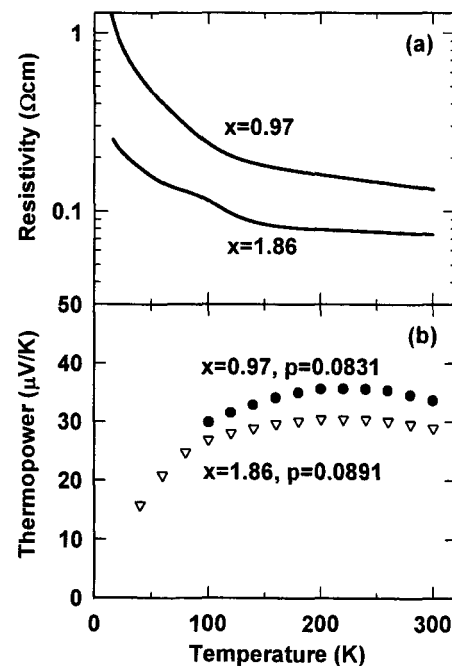


FIG. 2. Temperature dependence of (a) resistivity and (b) thermopower for Pb-3252 films.

nm. Additionally, the electronic structure calculations showed that the antibonding bands of Cu $3d_{x^2-y^2}$ and O $2p$ orbitals have similar in-plane dispersion for the Pb-3212, Pb-3222 and Pb-3232 phases.⁶

On the other hand, the electronic anisotropy was evaluated from the calculated energy bands,⁶ that is, from the ratio between Fermi velocities parallel and perpendicular to the CuO_2 plane. The anisotropy of Pb-3232 was larger than that of Pb-3212 by one order of magnitude.⁶ Therefore, the Pb-32 n 2 family is useful for changing the c -axis transport while the in-plane transport is kept constant. Utilizing this family, we tried to control the anisotropy of the superconductivity. The results are shown in the next section.

It should be noted that the temperature dependence of resistivity of the sample with $x=1.86$ in Fig. 2 shows an anomaly at 60 K to 80 K. A similar anomaly is occasionally seen in other samples at 60 K to 130 K. The origin is unknown.

3.2 [(Pb-32 n 2)₁(Pb-3212)₃]₉ superlattices

The XRD patterns of superlattices agreed well with the calculated patterns assuming the ideal crystal structure. The c -axis length of the samples increased by a unit length of 0.28 nm with increasing n , as expected. This shows that the distances between the superconducting layers are controlled at the shortest intervals so far achieved.

The temperature dependence of resistivity for [(Pb-32 n 2)₁(Pb-3212)₃]₉ with $n=1, 3, 4, 6$ was measured in an applied field parallel and perpendicular to the CuO_2 plane. Here, $n=1$ represents the Pb-3212 single-phase film with 36 unit-cell thickness. The current was parallel to the CuO_2 plane. We now discuss the changes in the resistive transition depending on n , from the following two points of view. Region I: the amplitude of the superconducting order parameter is small and fluctuations in the amplitude are crucial to the energy dissipation. Region II: the amplitude of the superconducting order parameter is well developed and the thermally activated flux flow (TAFF) dominates the energy dissipation.

Figure 3 shows the resistive transition under an applied field of 10 T perpendicular to the CuO_2 plane and in a zero field. In a zero field, resistivity for $n=3, 4$, and 6 exhibits its maximum at around 40 K, and then decreases with decreasing temperature, which indicates that the superconductivity starts to develop. In the magnetic field, the temperature width of region I, where resistivity is nearly the same as that of the normal state, say $\rho > 0.7\rho_N$, is expanded as n increases. This suggests that the fluctuations in the amplitude of order parameter under a magnetic field grow stronger with increasing n . The distance between superconducting layers, d_i , increases, as n increases. So the interlayer coupling is considered to become weak and, consequently, the two-dimensional fluctuations may be enhanced.

The activation energy for flux motion was estimated using the Arrhenius plots of the resistivity data in region II. The activation energy at $T=0$, U_0 , was calculated by using a relation⁷ $U_0=U(t)/(1-t^4)$ where $t=T/T_c$. In the case of the $H//\text{CuO}_2$ plane (Fig. 4), U_0 for the superlattices with $n=3-6$ has weaker field dependence than that of the Pb-3212 single-phase film ($n=1$) which shows U_0

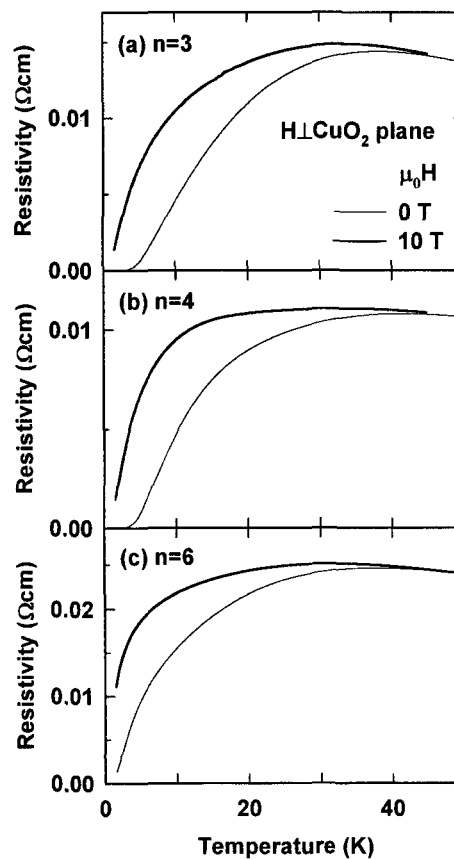


FIG. 3. Temperature dependence of resistivity for [(Pb-32 n 2)₁(Pb-3212)₃]₉ superlattices.

$\sim H^{-1/2}$. This reflects the small thickness of the superconducting layer in the superlattices.³ It should be noted that for the $H//\text{CuO}_2$ plane, the field-induced broadening of transition and hence a weak but finite field dependence of U_0 was observed at the field below H_{c1} ($\approx 30-40$ T), for the thin layer.³ These results indicate the existence of some interlayer couplings between the thin superconducting layers. The values of U_0 for both the perpendicular and parallel (Fig. 4) fields decrease with increasing n . This suggests that the interlayer coupling in the superconducting superlattices is weakened with increasing n , as explained in the following.

In the TAFF model, each individual flux line is pinned in a potential well and is depinned by thermal activation. The measured dissipation is related to the activation of the individual flux line. The activation energy U_0 is proportional to the correlation length, L_c , along the flux line. In the case of the $H\perp\text{CuO}_2$ plane, the pancake vortices move along the CuO_2 plane. As d_i increases, interaction between the pancake vortices on the adjacent superconducting layers becomes weak, resulting in a decrease of L_c and U_0 . Now, we compare the present system with the YBCO/PBCO superlattices, which have been thoroughly studied.^{3,8} In the case of YBCO/PBCO, the activation energy decreased with increasing PBCO thickness from 2.4 nm (2-unit cell) to 4.8 nm (4-unit cell).⁸ Thus, it is not surprising that U_0 decreases with increasing c -axis length of the Pb-32 n 2 phase from 2.13 nm ($n=3$) to 2.96 nm ($n=6$) in [(Pb-32 n 2)₁(Pb-3212)₃]₉ superlattices.

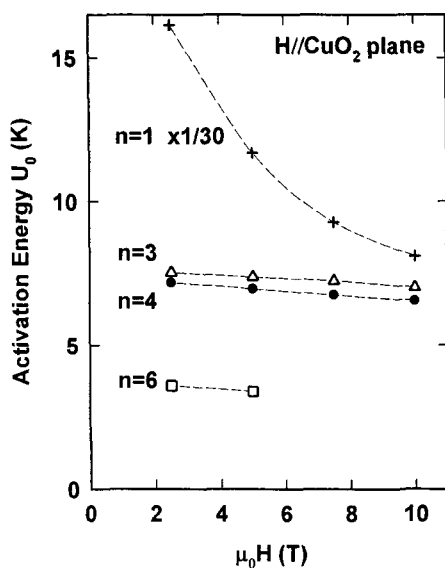


FIG. 4. Activation energies of flux motion for $[(\text{Pb-}32n2)_1(\text{Pb-}3212)_3]_9$ superlattices.

In the case of the $H//\text{CuO}_2$ plane, magnetic fluxes enter the insulating layers. The activation process corresponds to the flux jump across the CuO_2 plane, which is dominated by the creation of a pancake vortex-antivortex pair at the CuO_2 plane. The larger the distance d_i , the weaker the interlayer coupling is, resulting in a lowering of the energy barrier for the creation of the vortex-antivortex pair.

The experimental results show that the interlayer coupling of superconductivity is weakened as n increases. Therefore, what kind of interlayer coupling occurs has to be elucidated. Firstly, we should discuss the existence of the magnetic interlayer coupling, which has been studied as the origin of the dc transformer during the last quarter of the 20th century.⁹ In the case of YBCO/PBCO, the magnetic coupling was not observed since the energy of magnetic coupling was of the order of T_c and much lower than the observed activation energy.³ In the present case, U_0 was smaller by two orders of magnitude than YBCO/PBCO, and was of the order of T_c . So, we can expect to observe the magnetic coupling. The smaller U_0 may be caused by the stronger anisotropy in the Pb-3212 superconductor with rather low-doping and the fact that the T_c of the present samples was lower than those of YBCO. For more detail, we have to consider the field dependence for the energy of magnetic coupling. Following Ekin and Clem,⁹ the maximum coupling force can be written as:

$$F_m = \frac{3\phi_0^2}{32\pi^3\lambda^4} \frac{[1 - \exp(-g_{10}d_s)]^2 \exp(-g_{10}d_i)}{g_{10}^2}, \quad (1)$$

$$g_{10} = (8\pi^2 B / \sqrt{3}\phi_0)^{1/2}, \quad (2)$$

where λ , d_s , and d_i are the penetration depth, the thicknesses of the superconducting and insulation layer, respectively. The maximum coupling force occurs when the displacement of the vortex line is equal to one-fourth of the intervortex spacing, d_s . So, we estimated the maximum coupling energy, E_m to be $F_m d_s / 4$, which de-

creases with increasing H . In the perpendicular field less than 0.3 T, E_m is the order of the observed U_0 and there is the possibility of observing the magnetic coupling in the present system. However, in the perpendicular field larger than 2 T, E_m is smaller than one-tenth of the measured activation energy. Thus, there must be another coupling mechanism.

Secondly, we need to discuss whether the Josephson-like coupling exists or not. If the proximity effect (PE) acts on the CuO_2 planes in the Pb-32 n 2 phase with $n=3-6$, the Josephson-like coupling presumably exists between the thin superconducting layers. Previously, we investigated the possibility of the PE by comparing the transport properties of the Pb-32 n 2 phase with some theories.⁵ The sheet conductance per CuO_2 plane for the Pb-3252 phase showed that the present sample was near the border line for the occurrence of the PE, but we cannot deny the occurrence of the PE.⁵

4. SUMMARY

We tried to control an atomic layer structure and, consequently, the interlayer coupling of superconducting superlattices. The transport properties of the Pb-32 n 2 family were compared with the *ab initio* electronic structure calculations. Possible mechanisms for the low efficiency of hole doping were proposed: oxygen vacancies, or hole traps at the oxygen sites in the fluorite block. These are crucial to superconductivity in layered cuprates having a fluorite block. Using the Pb-32 n 2 family, we successfully grew the superconducting superlattices in which the distances between the superconducting layers were controlled at the shortest intervals so far achieved. The experimental results concerning the shape of resistive transition and the activation energy of flux motion indicated that the interlayer coupling across the fluorite block layer was controlled by changing the number of the atomic layer, n .

ACKNOWLEDGMENTS

This study was supported by the Special Coordination Funds for Promoting Science and Technology from the Japanese Science and Technology Agency, to which we are deeply indebted. We would like to thank Dr. H. Kubota of Toshiba Corporate R&D Center for illuminating discussion about vortex matter.

REFERENCES

- 1 R. Kleiner, F. Steinmeyer, G. Kunkel, and P. Müller, *Phys. Rev. Lett.*, **68**, 2394-2397 (1992).
- 2 S. Ikegawa and Y. Motoi, *Appl. Phys. Lett.* **68**, 2430-2432 (1996).
- 3 J. M. Triscone and Ø. Fischer, *Rep. Prog. Phys.* **60**, 1673-1721 (1997).
- 4 J. L. Tallon, C. Bernhard, H. Shaked, R. L. Hitterman and J. D. Jorgensen, *Phys. Rev. B* **51**, 12911-12914 (1995).
- 5 S. Ikegawa and Y. Motoi, *Phys. Rev. B* **61**, 6334-6342 (2000).
- 6 M. Arai and S. Ikegawa, this volume.
- 7 C. W. Hagen and R. Griessen, *Phys. Rev. Lett.* **62**, 2857-2860 (1989).
- 8 J.-M. Triscone et al., *Physica C* **185-189**, 210 (1991).
- 9 J. W. Ekin and J. R. Clem, *Phys. Rev. B* **12**, 1753-1765 (1975).